ELSEVIER

International Journal of Mass Spectrometry 190/191 (1999) 231–241

International Journal of Mass Spectrometry

Ion trap studies of $H^+(H_2SO_4)_m(H_2O)_n$ reactions with water, ammonia, and a variety of organic compounds

Edward R. Lovejoy*

NOAA Aeronomy Laboratory, 325 Broadway, Boulder, CO 80303, USA

Received 5 October 1998; accepted 31 December 1998

Abstract

Rate coefficients and products are reported for the reactions of protonated sulfuric acid and water clusters $H^+(H_2SO_4)_m(H_2O)_n$ with water, ammonia, and a variety of organic compounds. The cluster ions were generated in an external ion source and the reactions were studied in a quadrupole ion trap. These data yield the stabilities of $H^+H_2SO_4(H_2O)_{n=1-3}$. The implications of these results to the understanding of the role of H_2SO_4 in atmospheric ion chemistry are discussed. Effective internal temperatures of trapped $H^+(H_2O)_{n=3,4}$ and $H^+(NH_3)_3$ are also derived from kinetics of the unimolecular decomposition in the ion trap. (Int J Mass Spectrom 190/191 (1999) 231–241) © 1999 Elsevier Science B.V.

Keywords: Ion trap; Kinetics; Protonated sulfuric acid; Water clusters

1. Introduction

The mechanism for gas to particle conversion in the earth's atmosphere is not known. Field studies by Weber et al. [1] have demonstrated a correlation between gas phase sulfuric acid and ultrafine particles. The observed nucleation rates were significantly higher than predicted by theory for the binary sulfuric acid water system, and it was suggested that ammonia may be involved in the nucleation process. Despite the low atmospheric concentrations, ions may also play a role in nucleation [2] because the charge significantly stabilizes the small clusters relative to the neutral counterparts. Ion–ion recombination has also been suggested as a possible mechanism for new particle formation in the atmosphere [3]. Recently, Yu et al. showed that the rapid aerosol formation and growth observed in aircraft exhaust plumes is probably due to ions [4].

Ion concentrations in the troposphere and the lower and middle stratosphere are about 1000 cm^{-3} [5]. The dominant negative ions have the form $HSO_4^-(H_2SO_4)_x(HNO_3)_y$. Other core ions, e.g. $CH_3SO_3^-$ and $C_3H_3O_4^-$ are found in the troposphere. The positive ions are predominately $H^+CH_3CN(H_2O)_x$ and $H^+(H_2O)_x$ in the stratosphere. Strong bases like ammonia and pyridine are important positive ion constituents in the troposphere. The rates of ion-induced nucleation for atmospheric conditions are not known. The thermodynamics of cluster ions containing atmospheric species are needed to evaluate possible ion-induced nucleation mechanisms and rates. The purpose of the present study is to explore the stability and reactivity of positive cluster ions con-

* E-mail: nlovejoy@al.noaa.gov

Dedicated to J.F.J. Todd and R.E. March in recognition of their original contributions to quadrupole ion trap mass spectrometry.

PII S1387-3806(99)00006-8

taining H_2SO_4 and H_2O, two species implicated in the nucleation of atmospheric particles.

Viggiano et al. [6] have shown that sulfuric acid does not displace water from small protonated water clusters $H^+(H_2O)_{n=2-4}$, and postulated that H_2SO_4 does not play a significant role in stratospheric positive ion chemistry. The chemistry of the protonated sulfuric acid–water clusters is not known. In the present work the kinetics of reactions of protonated sulfuric acid–water clusters are studied. These data yield stabilities of the $H^+H_2SO_4(H_2O)_{n=1-3}$. An upper limit for the stability of the $H_2SO_4H_2O$ species is also derived from the data. Effective temperatures for trapped $H^+(H_2O)_{n=3,4}$ and $H^+(NH_3)_3$ are evaluated based on the kinetics of decomposition in the ion trap.

2. Experimental

The chemistry of protonated sulfuric acid–water clusters was studied with an ion–molecule reactor coupled to a quadrupole ion trap. The apparatus and methodologies used in the present study are the same as those described previously [7]. The rate coefficients for reactions of the ion clusters were measured in the quadrupole ion trap. The cluster ions were generated in a 1 m long by 3.4 cm inner diameter (i.d.) stainless steel ion–molecule reactor. Electrons were produced at the upstream end of the reactor with a hot thoriated iridium filament, and sulfuric acid and water vapor were added to the reactor downstream of the electron source. Maximum cluster ion signals were achieved with short reactor residence time, which reduced the consumption of the clusters via secondary ion chemistry. The reactor pressure was typically 0.7 Torr with a flow of about 100 STP $cm^3\ s^{-1}$ (STP = 273 K and 760 Torr) of He, giving residence times of about 5 ms. Sulfuric acid vapor was introduced into the reactor by flowing 5–20 STP $cm^3\ s^{-1}$ of He over about 0.5 cm^3 of hot concentrated H_2SO_4 (330–350 K) held in a stainless steel reservoir. The cluster ions were sampled through a 0.25 or 0.5-mm-diameter orifice at the downstream end of the ion–molecule reactor, and focused into the ion trap with a set of electrostatic lenses. The cluster ions were accumulated in the trap for 5–20 ms, isolated with a filtered noise field applied across the end caps, and then allowed to react for a variable reaction time. Kinetics were measured by monitoring the ion signals as a function of delay time for a range of reactant concentrations. Reactants were added directly to the ion trap chamber in a flow of He. The reactant/He flow was the major flow (>90%) into the ion trap chamber. All reactant flows except water and ammonia were determined by measuring the rate of change in pressure in a calibrated volume. The measured acetic acid flow rates were corrected for the presence of dimers based on the thermodynamics of dimerization reported by Buttner and Maurer [8]. The corrections were typically 30%. In the ammonia experiments an NH_3/He mixture flowed through a 50 cm long by 2.5-cm-diameter cell fitted with quartz windows, and the NH_3 concentration was determined by monitoring the absorption of the Hg 185 nm atomic line. An NH_3 absorption cross section of 4.2×10^{-18} cm^2 $molecule^{-1}$ was measured in the present work and agrees well with the cross section from Tannenbaum et al. [9]. In the water experiments the water concentration was determined by measuring the flow rate of a saturated H_2O/He stream added to the ion trap chamber. He flowed through a glass frit submerged in liquid water, and the saturated water stream flowed through a mass flow meter and into the ion trap chamber. The water temperature and the pressure in the bubbler were measured to determine the water vapor mixing ratio. All other gas flows were measured with mass flowmeters calibrated by measuring the rate of pressure change in calibrated volumes. The concentration of reactant in the ion trap was calculated as described previously, with correction for mass dependent conductance of the trap chamber [7]. Pressures were measured with capacitance manometers.

3. Results

Kinetics of the cluster reactions were determined by monitoring the decay of the ion signal as a function of reaction time for a range of reactant concentrations. As an example, a set of decay curves for the reaction

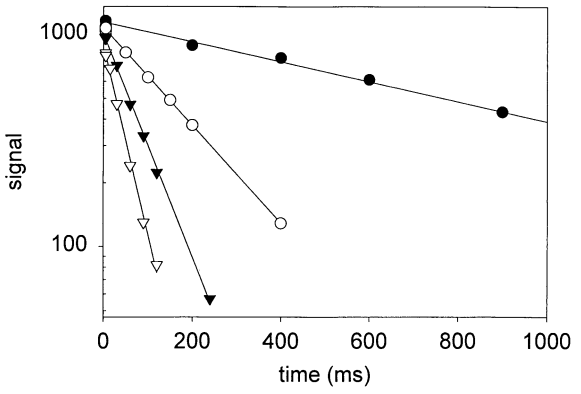

Fig. 1. Variation of $H^+H_2SO_4$ signal as a function of reaction time for a range of [CH_3CN]. [CH_3CN] = 0.0 (filled circles), 1.0 (open circles), 2.9 (filled triangles), and 5.3 × 10^9 molecule cm^{-3} (open triangles).

$H^+H_2SO_4$ + CH_3CN are shown in Fig. 1. The slopes of these decays give the pseudo-first-order rate coefficients. Pseudo-first-order rate coefficients are plotted as a function of the CH_3CN concentration in Fig. 2 for $H^+H_2SO_4(H_2O)_{n=0-2}$. The slopes of these plots yield the second-order rate coefficients. The second-order rate coefficients for reactions of $H^+(H_2O)_{n=2,3}$ and $H^+H_2SO_4(H_2O)_{n=0-2}$ with a series of organic reactants are listed in Tables 1–5. The rate coefficients are estimated to be accurate to ±20% unless specified otherwise. All the kinetics experiments were conducted in 1.0 ± 0.05 mTorr He. The kinetics of the $H^+(H_2O)_n$ and $H^+H_2SO_4(H_2O)_n$ reactions were measured with trapping voltages of 236 and 456 V_{p-p}, respectively. The ion trap stability parameter q_z is given by 0.0479 V_{p-p}/m, where V_{p-p} is the peak-to-peak rf voltage and m is the ion mass in amu. The rate coefficient for $H^+(H_2O)_2$ + CH_3OH was independent (<5% change) of the trapping voltage in the range 236−456 V_{p-p}. All rate coefficients were measured by monitoring the disappearance of the reactant ion, except for the reaction $H^+H_2SO_4H_2O$ + acetone. In this reaction the secondary product ion $H^+(CH_3C(O)CH_3)_2$ has the same mass as $H^+H_2SO_4H_2O$, and the rate coefficient was measured by monitoring the appearance of the $H^+CH_3C(O)CH_3$ ion. The $H^+H_2SO_4$ + $CH_3C(O)CH_3$ reaction kinetics were measured by monitoring the decay of $H^+H_2SO_4$ and the appearance of $H^+CH_3C(O)CH_3$. Both approaches gave the same rate coefficient within 5%.

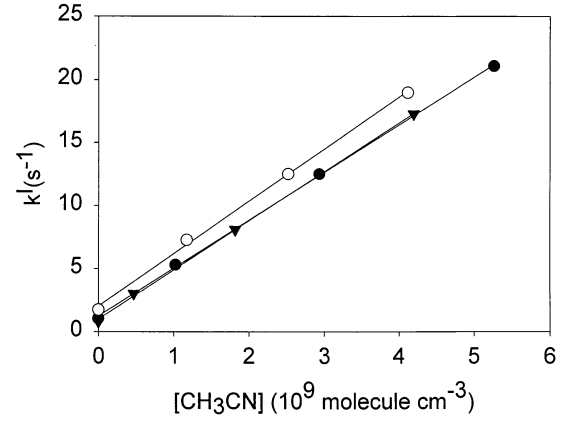

Fig. 2. Pseudo-first-order rate coefficients for the reactions of $H^+H_2SO_4$ (filled circles), $H^+H_2SO_4H_2O$ (open circles), and $H^+H_2SO_4(H_2O)_2$ (filled triangles) with CH_3CN as a function of [CH_3CN].

Collision rate coefficients were calculated for the cluster ion reactions by using the method described by Su and Chesnavich [10]. Molecular polarizabilities and dipole moments were taken from [11] and [12], respectively. The calculated collision rate coefficients at 300 K are listed in Tables 1–5.

Product yields listed in Tables 1–5 are the fractional ion signals at small reactant ion conversion (<30%). The product ion yields are estimated to be accurate to about ±30% of the yield. The main sources of uncertainty are possible mass discrimination and secondary chemistry.

The unimolecular decompositions of several of the cluster ions were also studied in the ion trap. Decomposition rate consants for the $H^+(H_2O)_{n=3,4}$, $H^+(NH_3)_3$, and $H^+H_2SO_4(H_2O)_3$ ions are listed in Table 6. Assuming that the internal energy of the trapped ion is partitioned according to a Boltzmann distribution, the ion decomposition rate coefficient is given by [7]

$$k_d = \frac{k_a \exp\left(\frac{\Delta S^o}{R}\right) \exp\left(\frac{-\Delta H^o}{RT}\right)}{1.362 \times 10^{-22} T} \quad (1)$$

Table 1
Kinetics and products of $H^+(H_2O)_2$ reactions

Reactant	Mass	Rate constants[a] (10^{-9} cm^3 molecule^{-1} s^{-1})	Product masses	Product yields
Methanol CH_3OH	32	2.8	33	<0.02
		[19] 2.4 ± 0.6	51	>0.98
		[24] 1.8 ± 0.5		
		[23] 1.8 ± 0.7		
		(2.3)		
Ethanol C_2H_5OH	46	2.6	47	<0.02
		[19] 2.5 ± 0.6	65	>0.98
		(2.2)		
Acetonitrile CH_3CN	41	4.4	42	<0.02
		[24] 3.0 ± 0.9	60	>0.98
		[22] 4.0 ± 1.2		
		[25] 4.0 ± 0.8		
		(4.2)		
Cyclohexene C_6H_{10}	82	1.2	83	0.45
		(1.7)	101	0.55
Toluene C_7H_8	92	0.8	93	>0.98
		(1.7)	111	<0.02
o-xylene C_8H_{10}	106	2.6	107	>0.98
		(1.9)	125	<0.02
Acetone C_3H_6O	58	2.8	59	0.66
		[19] 3.5 ± 0.9	77	0.34
		[24] 2.3 ± 0.7		
		(3.2)		
Ammonia NH_3	17	1.9	18	>0.97, [19] 1.0
		[19] 2.0 ± 0.4	36	<0.03
		[24] 1.7 ± 0.5		
		[20] 2.2 ± 0.4		
		[21] 2.6 ± 0.8		
		(2.3)		

[a] Collision rate coefficients are listed in parentheses.

Table 2
Kinetics and products of $H^+(H_2O)_3$ reactions

Reactant	Mass	Rate constants[a] (10^{-9} cm^3 molecule^{-1} s^{-1})	Product masses	Product yields
Acetone C_3H_6O	58	2.5	59	<0.02
		[19] 3.0 ± 0.8	77	>0.95
		[24] 2.2 ± 0.7	95	<0.03
		(2.8)		
Ammonia NH_3	17	1.7	18	<0.02
		[19] 1.9 ± 0.4	36	>0.96, [24] 1.0
		[20] 2.3 ± 0.5	54	<0.02
		[21] 1.6 ± 0.5		
		(2.2)		

[a] Collision rate coefficients are listed in parentheses.

Table 3
Kinetics and products of $H^+H_2SO_4$ reactions

Reactant	Mass	Rate constants[a] (10^{-9} cm^3 molecule^{-1} s^{-1})	Product masses	Product yields
Water H_2O	18	0.09	37	
		(2.3)		
Methanol CH_3OH	32	2.9	33	
		(1.9)		
Benzene C_6H_6	78	1.4	79	
		(1.2)		
Acetaldehyde CH_3COH	44	2.6	45	
		(2.5)		
Ethanol C_2H_5OH	46	2.2	47	
		(1.8)		
Allene CH_2CCH_2	40	1.1	41	0.70
		(1.1)	59	0.30
Acetonitrile CH_3CN	41	3.8	42	
		(3.4)		
Cyclohexene C_6H_{10}	82	1.4	83	
		(1.3)		
Acetic acid CH_3COOH	60	2.6	61	
		(1.7)		
Toluene C_7H_8	92	1.4	93	
		(1.3)		
Isopropanol $CH_3CH(OH)CH_3$	60	2.4	43	0.40
		(1.7)	61	0.60
o-xylene C_8H_{10}	106	1.5	107	
		(1.4)		
Acetone $(CH_3)_2CO$	58	2.9	59	
		(2.5)		
Ammonia NH_3	17	1.5	18	
		(2.1)		

[a] Collision rate coefficients are listed in parentheses.

where k_d is the ion decomposition rate constant, k_a is the association rate coefficient for the reverse reaction, and ΔS^o and ΔH^o are the entropy and enthalpy changes for the decomposition reaction. k_d and k_a have molecular units (i.e. k_d/k_a = molecule cm^{-3}). Effective ion temperatures were calculated for $H^+(H_2O)_{n=3,4}$ and $H^+(NH_3)_3$ based on published thermochemistry [13,14] and association rate constants [15,16], using Eq. (1).

4. Discussion

4.1. Effective temperatures of trapped cluster ions

The second-order decomposition rate coefficient measured for $H^+(H_2O)_4$ is about one half of the value reported by McLuckey et al. [17] at 1.2 mTorr He. The limit on the $H^+(H_2O)_3$ decomposition rate coefficient measured in the present work is consistent with values measured by McLuckey et al. [17] at lower pressure. In the present work the second-order decomposition rate coefficients for $H^+(H_2O)_4$ and $H^+(NH_3)_3$ were independent of the ion trap pressure over the range 0.1–1.0 mTorr He. In contrast, McLuckey et al. [17] reported that the second-order decomposition rate coefficients for $H^+(H_2O)_n$ and $H^+(CH_3OH)_n$ decreased as the pressure was increased over the range 0.02–1.2 mTorr.

The effective internal temperatures of $H^+(H_2O)_{n=3,4}$ and $H^+(NH_3)_3$ derived from the trap decay rates are all close to the actual trap temperature. This is the same conclusion that was drawn for the $NO_3^-(HNO_3)_2$

Table 4
Kinetics and products of $H^+H_2SO_4H_2O$ reactions

Reactant	Mass	Rate constants[a] (10^{-9} cm^3 molecule^{-1} s^{-1})	Product masses	Product yields
Water H_2O	18	0.4	37	
		(2.3)		
Methanol CH_3OH	32	2.6	33	<0.02
		(1.9)	51	0.48
			131	0.52
Benzene C_6H_6	78	<0.04		
		(1.1)		
Acetaldehyde CH_3COH	44	2.7	45	<0.03
		(2.4)	63	0.64
			143	0.36
Ethanol C_2H_5OH	46	2.4	47	<0.01
		(1.7)	65	0.54
			145	0.46
Allene CH_2CCH_2	40	0.8	41	<0.01
		(1.1)	43	0.10
			59	0.51
			77	0.18
			139	0.21
Acetonitrile CH_3CN	41	4.2	42	<0.02
		(3.3)	60	0.82
			140	0.18
Cyclohexene C_6H_{10}	82	1.3	83	0.84
		(1.2)	101	0.16
Acetic acid CH_3COOH	60	3.0	61	0.14
		(1.6)	79	0.56
			159	0.30
Toluene C_7H_8	92	1.3	93	
		(1.2)		
Isopropanol $CH_3CH(OH)CH_3$	60	2.6	61	0.28
		(1.7)	79	0.43
			159	0.29
o-xylene C_8H_{10}	106	1.8	107	
		(1.3)		
Acetone $(CH_3)_2CO$	58	3.1	59	0.68
		(2.4)	77	0.26
			157	0.06
Ammonia NH_3	17	1.6	18	0.97
		(2.1)	36	0.03
			116	<0.05

[a] Collision rate coefficients are listed in parentheses.

ion in previous work [7] with the same apparatus. Based on these measurements a value of 330 ± 30 K is adopted for the effective internal temperature of the cluster ions in the present work. This value is consistent with recent measurements by Gronert [18] who reported an effective trapped ion temperature of 310 ± 20 K based on measured equilibrium constants for the association of thiophenolate and 2,2,2-trifluoroethanol.

4.2. $H^+(H_2O)_2$ reactions

The rate coefficients for the reaction of $H^+(H_2O)_2$ with CH_3OH, C_2H_5OH, CH_3CN, $(CH_3)_2CO$, and NH_3 are in good agreement with previous flowing afterglow measurements [19–25] (see Table 1). Rate coefficients were measured for reactions of $H^+(H_2O)_2$ with a series of organic molecules in order to bracket the threshold for direct proton transfer

Table 5
Kinetics and products of $H^+H_2SO_4(H_2O)_2$ reactions

Reactant	Mass	Rate constants[a] (10^{-9} cm^3 molecule^{-1} s^{-1})	Product masses	Product yields
Water H_2O	18	0.3	55	
		(2.3)		
Methanol CH_3OH	32	2.6	69	0.31
		(1.8)	149	0.69
Benzene C_6H_6	78	<0.07		
		(1.1)		
Ethanol C_2H_5OH	46	2.5	47	<0.03
		(1.7)	83	0.34
			145	0.14
			163	0.52
Allene CH_2CCH_2	40	<0.04		
		(1.1)		
Acetonitrile CH_3CN	41	3.9	42	<0.02
		(3.3)	60	0.49
			78	0.36
			158	0.15
Cyclohexene C_6H_{10}	82	0.3	[b]	
		(1.2)		
Acetic acid CH_3COOH	60	2.8	79	0.30
		(1.6)	97	0.24
			159	0.16
			177	0.30
Toluene C_7H_8	92	<0.1		
		(1.2)		
Isopropanol $CH_3CH(OH)CH_3$	60	2.4	79	0.40
		(1.6)	159	0.38
			177	0.22
o-xylene C_8H_{10}	106	<0.2		
		(1.3)		
Acetone $(CH_3)_2CO$	58	2.7	59	<0.04
		(2.4)	77	0.85
			157	0.15
Ammonia NH_3	17	1.7	18	<0.02
		(2.1)	36	0.30
			116	0.70
			134	<0.05

[a] Collision rate coefficients are listed in parentheses.
[b] Products are uncertain due to secondary chemistry.

$$H^+(H_2O)_2 + X \rightarrow XH^+ + H_2O + H_2O \quad (2)$$

Two water molecules are probably produced at the proton transfer threshold because the reaction

$$(H_2O)_2 \rightarrow H_2O + H_2O \quad (3)$$

is exergonic at the temperature of the trap (ΔH^o = 3.6 kcal mol^{-1}, ΔS^o = 0.019 kcal mol^{-1} K^{-1} [26]). The threshold for $H^+(H_2O)_2$ proton transfer is bracketed by acetonitrile and cyclohexene (see Table 1). The proton transfer reaction may be written as a sum of reactions

$$X + H^+ \rightarrow XH^+ \quad (4)$$

$$H^+H_2O \rightarrow H^+ + H_2O \quad (5)$$

$$H^+(H_2O)_2 \rightarrow H^+H_2O + H_2O \quad (6)$$

$$\text{net:} \quad H^+(H_2O)_2 + X \rightarrow XH^+ + H_2O + H_2O \quad (2)$$

Table 6
Cluster ion decomposition kinetics

Reaction	Decomposition rate constant (cm^3 $molecule^{-1}$ s^{-1}) and pressure (mTorr)	Association rate constants (cm^6 $molecule^{-2}$ s^{-1}), ΔH (kcal mol^{-1}), and ΔS (kcal mol^{-1} K^{-1})	Ion temperature[b] (K)
$H^+(H_2O)_3 + He \rightarrow$	$<2 \times 10^{-15}$	1.5×10^{-27} [15]	$H^+(H_2O)_3$
$H^+(H_2O)_2 + H_2O + He$	1.5	−19.5 [13]	<358 K
		−0.022 [13]	
$H^+(H_2O)_4 + He \rightarrow$	4.2×10^{-14}	1.5×10^{-27} [15]	$H^+(H_2O)_4$
$H^+(H_2O)_3 + H_2O + He$	0.2–1.1	−17.5 [13]	324 ± 30 K
		−0.027 [13]	
$H^+(NH_3)_3 + He \rightarrow$	1.7×10^{-14}	1.3×10^{-27} [16][a]	$H^+(NH_3)_3$
$H^+(NH_3)_2 + NH_3 + He$	0.1–1.0	−17.5 [14]	340 ± 30 K
		−0.023 [14]	
$H^+H_2SO_4(H_2O)_3 + He \rightarrow$	2.5×10^{-13}		
$H^+H_2SO_4(H_2O)_2 + H_2O + He$	0.5		
$H^+H_2SO_4(H_2O)_3 + He \rightarrow$	$<3 \times 10^{-14}$		
$H^+(H_2O)_3 + H_2SO_4 + He$	0.5		

[a] He third body efficiency estimated.
[b] Uncertainty based on estimated uncertainties of ±1 kcal mol^{-1} in ΔG^o and a factor of 2 in the equilibrium constant.

and the thermodynamics for the proton transfer reaction may be calculated based on published thermodynamics for reactions (4)–(6). Reaction (2) is predicted to be endothermic by 10–16 kcal mol^{-1} for X representing a species with a proton affinity that is the average of that for acetonitrile and cyclohexene. Proton affinities for water, acetonitrile, and cyclohexene are from the tabulation by Hunter and Lias [27] and are listed in Table 7. Literature values for the H^+H_2O–H_2O bond enthalpy range from 32–38 kcal mol^{-1} [13,28–33]. The proton transfer reaction between $H^+(H_2O)_2$ and X is endothermic by 6–12 kcal mol^{-1} if the water dimer is the product of reaction (2). It is unlikely that the energy of the trapped ions is sufficient to overcome these large endothermicities. Note that direct proton transfer is not observed between $H^+H_2SO_4$ and water, a reaction that is only 2 kcal mol^{-1} endothermic. It is more likely that the $H^+(H_2O)_2$ proton transfer threshold is determined by the Gibbs free energy change for the reaction. By using the published gas phase basicities [27] for water, acetonitrile, and cyclohexene, and published ΔH^o and ΔS^o values for reaction (6) [13,31–33] it is found that a reaction temperature in the range 330–450 K is required to give $\Delta G^o = 0$ for reaction (2). These temperatures are higher than the expected internal temperature of the ions. Ion translational excitation may account for the difference between the internal temperature and the effective reaction temperature.

4.3. $H^+(H_2O)_3$ reactions

$H^+(H_2O)_3$ reacts with acetone and ammonia at the collision frequency, consistent with previous studies [19–21,24]. The major products are $H^+CH_3(CO)CH_3(H_2O)$ and $H^+(NH_3)(H_2O)$. No direct proton transfer products are observed.

4.4. $H^+H_2SO_4$ reactions

$H^+H_2SO_4$ reacts by simple proton transfer at the collision rate with all of the reactants having a proton affinity larger than H_2SO_4 [27]. $H^+H_2SO_4$ reacts at only about 4% of the collision rate with water

$$H^+H_2SO_4 + H_2O \rightarrow H^+(H_2O)_2 + SO_3 \quad (7)$$

However, this is not a simple proton transfer or ligand switching reaction. Elimination of SO_3 may introduce a barrier, leading to a reduced rate coefficient, even though the reaction is exergonic by about 9 kcal

Table 7
Proton transfer thermodynamic parameters[a]

M	PA(M, 298K) (kcal mol^{-1})	ΔS_p(M, 298K) (cal mol^{-1} K^{-1})	GB(M, 330K) (kcal mol^{-1})
Water H_2O	165.2	1	157.0
Sulfuric acid H_2SO_4	167.2	0	158.6
Methanol CH_3OH	180.3	2	172.4
Benzene C_6H_6	179.4	6	172.8
Acetaldehyde CH_3COH	183.7	0.4	175.2
Allene CH_2CCH_2	185.3	2	177.5
Ethanol C_2H_5OH	185.6	2	177.5
Acetonitrile CH_3CN	186.2	1	178.0
Cyclohexene C_6H_{10}	187.5	0	178.9
Acetic acid CH_3COOH	187.3	1	179.1
Toluene C_7H_8	187.4	4	180.1
Isopropanol $CH_3CH(OH)CH_3$	189.5	2	181.5
o-xylene C_8H_{10}	190.3	4	182.9
Acetone $(CH_3)_2CO$	194.1	2	186.2
Ammonia NH_3	204.0	−2	194.9

[a] Data from [27] with the following definitions:
PA(M, T) = $\Delta H^o(MH^+ \rightarrow M + H^+)(M, T)$
$\Delta S_p(M, T) = S^o(MH^+, T) - S^o(M, T)$
$GB(M, T) = \Delta G^o(MH^+ \rightarrow M + H^+)(M, T) = PA(M, T) + T(\Delta S_p(M, T) - S^o(H^+, T))$
$S^o(H^+, 298K) = 26.0$ cal mol^{-1} K^{-1}

mol^{-1}. Some interesting reaction products are observed in the $H^+H_2SO_4$ reactions with allene and isopropanol. A significant fraction of allene is hydrated producing a mass 59 ion (protonated acetone or allyl alcohol) plus SO_3. In the isopropanol reaction, the alcohol is dehydrated and protonated propene is observed as a significant product.

4.5. $H^+H_2SO_4(H_2O)_{n=1-3}$ reactions

The $H^+H_2SO_4(H_2O)_n$ reactions mostly proceed at the collision frequency by simple ligand switching and/or direct proton transfer. Some notable exceptions are the reactions with water. The rate constants for the simple ligand switching reactions with water are less than collisional:

$$H^+H_2SO_4H_2O + H_2O \rightarrow H^+(H_2O)_2 + H_2SO_4 \quad (8)$$

$$H^+H_2SO_4(H_2O)_2 + H_2O \rightarrow H^+(H_2O)_3 + H_2SO_4 \quad (9)$$

$$H^+H_2SO_4(H_2O)_3 + H_2O \rightarrow H^+(H_2O)_4 + H_2SO_4 \quad (10)$$

($k_8 = 4 \times 10^{-10}$, $k_9 = 3 \times 10^{-10}$, $k_{10} = 1 \times 10^{-10}$ cm^3 $molecule^{-1}$ s^{-1}) suggesting that the binding of sulfuric acid to the protonated water clusters is equivalent to or weaker than the binding of water to the same cluster.

A distinct threshold is observed for $H^+H_2SO_4H_2O$ proton transfer. The threshold is bracketed by acetonitrile and cyclohexene (see Table 4), similar to $H^+(H_2O)_2$. Assuming that $H^+H_2SO_4H_2O$ proton transfer produces $H_2SO_4 + H_2O$, and the threshold is dictated by the Gibbs free energy change, then the Gibbs free energy change for the ligand switching reaction between $H^+H_2SO_4H_2O$ and H_2O (8) can be written as the sum of the $H^+H_2SO_4H_2O$ and $H^+(H_2O)_2$ proton transfer threshold reactions

$$H^+H_2SO_4H_2O + X \rightarrow XH^+ + H_2SO_4 + H_2O \quad \Delta G^o = 0.0 \pm 1.0 \text{ kcal mol}^{-1} \quad (11)$$

$$XH^+ + H_2O + H_2O \rightarrow H^+(H_2O)_2 + X \quad \Delta G^o = 0.0 \pm 1.0 \text{ kcal mol}^{-1} \quad (-2)$$

net: $H^+H_2SO_4H_2O + H_2O$

$\rightarrow H^+(H_2O)_2 + H_2SO_4$

$\Delta G^o = 0 \pm 1.4$ kcal mol^{-1} (8)

where X represents a species with a gas phase basicity between that of acetonitrile and cyclohexene. This analysis predicts that the ligand switching reaction between $H^+H_2SO_4H_2O$ and H_2O is close to ergoneutral. This result is consistent with the observation that reaction (8) is slow, and supports the assumption that H_2SO_4 and H_2O are the products at the $H^+H_2SO_4H_2O$ proton transfer threshold. This conclusion may also imply a limit on the stability of the neutral complex $H_2SO_4H_2O$. If the cluster $H_2SO_4H_2O$ was more stable than $H_2SO_4 + H_2O$, then the threshold for proton transfer from $H^+H_2SO_4H_2O$ would be lower than that for producing $H_2SO_4 + H_2O$. The fact that the proton transfer threshold coincides with production of $H_2SO_4 + H_2O$ suggests that $H_2SO_4H_2O$ is less stable than $H_2SO_4 + H_2O$, i.e. $\Delta G^o_{400K} \leq 0$ kcal mol^{-1} for the reaction

$$H_2SO_4H_2O \rightarrow H_2SO_4 + H_2O \quad (12)$$

Here it is assumed that the effective reaction temperature is about 400 K, based on the results for the $H^+(H_2O)_2$ proton transfer threshold. By using an entropy change for reaction (12) of 0.030 kcal mol^{-1} K^{-1} [34] a limit of $\Delta H^o \leq 12$ kcal mol^{-1} is derived. This is smaller than the liquid drop value reported by Mirabel and Ponche [35] ($\Delta H^o = 14$ kcal mol^{-1}), but comparable to the ab initio value from Morokuma and Muguruma [36] ($\Delta H^o = 11$ kcal mol^{-1}) and the density functional value from Bandy and Ianni [34] ($\Delta H^o = 10$ kcal mol^{-1}).

$H^+H_2SO_4(H_2O)_2$ does not react efficiently with the unsaturated species, benzene, allene, cyclohexene, toluene, and o-xylene. Conversely $H^+H_2SO_4(H_2O)_2$ reacts at the collision rate by ligand switching reactions with all the polar reactants. Channels leading to the elimination of single water and H_2SO_4 molecules as well as the elimination of two waters and water plus H_2SO_4 are observed. The elimination of two ligands is dominant in the more exothermic reactions with the most basic reactants, e.g. acetone and ammonia.

5. Atmospheric implications

The observation that H_2O displaces H_2SO_4 from $H^+H_2SO_4(H_2O)_{n=1-3}$ is consistent with the report by Viggiano et al. [6] that the reverse reactions are slow, i.e. H_2SO_4 does not react with $H^+(H_2O)_{n=2-4}$. Both observations support the conclusion that H_2SO_4 does not incorporate significantly into the small protonated water clusters in the earth's atmosphere. The observed trend of decreasing reaction rate coefficients with increasing cluster size for the ligand switching reactions $H^+H_2SO_4(H_2O)_{n=1-3} + H_2O \rightarrow H^+(H_2O)_{n+1} + H_2SO_4$ is probably due to an increase in the binding of sulfuric acid relative to water as the cluster size increases. This postulate is also supported by the observation that $H^+H_2SO_4(H_2O)_3$ decomposes in the ion trap by eliminating H_2O and not H_2SO_4. It is likely that the larger water clusters ($H^+(H_2O)_{n>4}$) will bind H_2SO_4 more strongly than H_2O, and H_2SO_4 may incorporate into the larger protonated water clusters in the stratosphere. The thermodynamics for the formation of larger protonated water and sulfuric acid clusters are needed in order to evaluate the role of ions in the nucleation of stratospheric aerosol.

Acknowledgements

Valuable assistance from Rob Wilson and useful discussions with Greg Huey, Dave Hanson, and Carl Howard are acknowledged. This work was supported in part by NOAA's Health of the Atmosphere Initiative.

References

[1] R.J. Weber, P.H. McMurry, F.L. Eisle, D.J. Tanner, J. Atmos. Sci. 52 (1995) 2242.
[2] See, e.g. A.W. Castleman Jr., P.M. Holland, R.G. Keesee, J. Chem. Phys. 68 (1978) 1760.
[3] F. Arnold, Nature 284 (1980) 610.
[4] F. Yu, R.P. Turco, B. Karcher, F.P. Schroeder, Geophys. Res. Lett. 25 (1998) 3839.
[5] A.A. Viggiano, Mass Spectrom. Rev. 12 (1993) 115.
[6] A.A. Viggiano, R.A. Perry, D.L. Albritton, E.E. Ferguson, F.C. Fehsenfeld, J. Geophys. Res. 85 (1980) 4551.
[7] E.R. Lovejoy, R.R. Wilson, J. Phys. Chem. 102 (1998) 2309.

[8] R. Buttner, G. Maurer, Ber. Bunsenges. Phys. Chem. 87 (1983) 877.
[9] E. Tannenbaum, E.M. Coffin, A.J. Harrison, J. Chem. Phys. 21 (1953) 311.
[10] T. Su, W.J. Chesnavich, J. Chem. Phys. 76 (1982) 5183.
[11] T.M. Miller, in CRC Handbook of Chemistry and Physics, 70th edition, R.C. Weast (Ed.), CRC, Boca Raton, FL, 1989.
[12] R.D. Nelson Jr., D.R. Lide Jr., A.A. Maryott, National Standard Reference Data Series, National Bureau of Standards-10, 1967.
[13] A.J. Cunningham, J.D. Payzant, P. Kebarle, J. Am. Chem. Soc. 94 (1972) 7627.
[14] J.D. Payzant, A.J. Cunningham, P. Kebarle, Can. J. Chem. 51 (1973) 3242.
[15] V.M. Bierbaum, M.F. Golde, F. Kaufman, J. Chem. Phys. 65 (1976) 2715.
[16] L.J. Puckett, M.W. Teague, J. Phys. Chem. 54 (1971) 4860.
[17] S.A. McLuckey, G.L. Glish, K.G. Asano, J.E. Bartmess, Int. J. Mass Spectrom. Ion Processes 109 (1991) 171.
[18] S. Gronert, J. Am. Soc. Mass Spectrom. 9 (1998) 845.
[19] D.K. Bohme, G.I. Mackay, S.D. Tanner, J. Am. Chem. Soc. 101 (1979) 3724.
[20] D. Smith, N.G. Adams, M.J. Henchman, J. Chem. Phys. 72 (1980) 4951.
[21] F.C. Fehsenfeld, E.E. Ferguson, J. Chem. Phys. 59 (1973) 6272.
[22] D. Smith, N.G. Adams, E. Alge, Planet. Space Sci. 29 (1981) 449.
[23] F.C. Fehsenfeld, I. Dotan, D.L. Albritton, C.J. Howard, E.E. Ferguson, J. Geophys. Res. 83 (1978) 1333.
[24] A.A. Viggiano, F. Dale, J.F. Paulson, J. Chem. Phys. 88 (1988) 2469.
[25] X. Yang, A.W. Castleman Jr., J. Chem. Phys. 95 (1991) 130.
[26] L.A. Curtis, D.J. Frurip, M. Blander, J. Chem. Phys. 71 (1979) 2703.
[27] E.P.L. Hunter, S.G. Lias, J. Phys. Chem. Ref. Data 27 (1998) 413.
[28] K. Honma, L.S. Sunderlin, P.B. Armentrout, Int. J. Mass Spectrom. Ion Processes 117 (1992) 237.
[29] N.F. Dalleska, K. Honma, P.B. Armentrout, J. Am. Chem. Soc. 115 (1993) 12 125.
[30] K. Honma, L.S. Sunderlin, P.B. Armentrout, J. Chem. Phys. 99 (1993) 1623.
[31] M. Meot-Ner, F.H. Field, J. Am. Chem. Soc. 99 (1977) 998.
[32] M. Meot-Ner, C.V. Speller, J. Phys. Chem. 90 (1986) 6616.
[33] K. Hiraoka, H. Takimoto, S. Yamabe, J. Phys. Chem. 90 (1986) 5910.
[34] A.R. Bandy, J.C. Ianni, J. Phys. Chem. 102 (1998) 6533.
[35] P. Mirabel, J.L. Ponche, Chem. Phys. Lett. 183 (1991) 21.
[36] K. Morokuma, C. Muguruma, J. Am. Chem. Soc. 116 (1994) 10 316.